

The Effect of Image Resolution on the Geometric Correction of Remote Sensing Satellite Images

Mohamed Tawfik, Hassan Elhifnawy, Ayman Ragab, Essam Hamza

Abstract—Geometric distortion due to sensor and/or environmental error sources represent a big problem in the final reported accuracy of captured satellite images. Image to image registration is one of commonly used processes of geometric correction of captured images for updating digital maps and GIS databases. This research tested the effect of different raw image resolutions with respect to reference image resolution on accuracy of image registration process. The research algorithm is implemented using different resolution satellite images from two different sensors, IKONOS and LANDSAT8. The reference data is an image of 1.0meter resolution from IKONOS-2 satellite images. Spatial interpolation process is applied using first order polynomial technique with four ground control points from reference image, which are sharp defined and well distributed. Nearest neighbour technique is used for investigating intensity pixel values of resultant new corrected images.

Geometric correction gave accurate results when using raw images with resolution same or higher than the reference image. The resolution of raw available images may be selected based on the required applications. Images with resolution lower than reference image can be used with applications that do not need high accuracy.

Index Terms—Geometric distortions, Geometric Correction, Image Resolution.

I. INTRODUCTION

The problem with all satellite images is that raw remotely sensed imagery often contains geometric distortions. Geometric distortion is defined as in accurate location of features in the image with respect to their accurate positions in the ground. Image distortion can be found due to different sources, effect of tilt of capturing angle, sensor lens distortion, the atmosphere refraction and earth curvature [1][2]. Lack of sensor calibration information and precise ephemeris data is considered as a big problem for applying the precise mathematical models for geometric correction. Fulfilling the required accuracy of registered images without any information about the sources of error needs more processes and computations. Geometric correction is an important process for producing georeferenced remote sensing images that can be used to extract accurate spatial data about features as distances, areas and coordinates. These data are necessary for many applications as change detection, object tracking, map production, feature measurements and environment surveillance [3]. Geometric correction is a vital process for preparing a remotely sensed data free or partially free of geometric distortion depending on the accuracy of

correction process, to make each individual pixel in the image in their proper planimetric (x, y) location. There are two strategies for geometric correction based on available data. The first strategy is a rigorous physical model that requires knowledge of the sensor parameters, also knowledge about sources of distortion to perform corresponding correction formulae [4] [5]. The second strategy is empirical models, which require the availability of reference known georeferenced data as Ground Control Points (GCPs), rectified image (corrected before) as a reference one or a map to be used for transformation process [2] [5] [4]. The second strategy is the most commonly used because it is independent of the used platform for image acquisition or not requires any information about sensor used for acquisition process [2] [5].

Geometric correction contains two main operations to be performed, coordinate transformation and pixel value determination. The first operation is the transformation process between two images (raw and reference) images. This operation can be performed by using Ground Control Points (GCPs) to build a mathematical relation for getting the transformation parameters, this operation known as a spatial interpolation. The second operation is the intensity determination to calculate the pixel value which is a new Digital Number (DN) in the corrected image that is calculated from the original DN values of the reference image this operation known as an intensity interpolation [3] [6] [7].

The image spatial resolution is the capability of the sensor to observe or measure the smallest object clearly with distinct boundaries and it is represented by pixel which is actually a unit of the digital resolution. Spatial resolution depends on properties and specifications of image production system (sensor) [8] [9]. Image resolution can be changed by generating images with different width and /or height in pixels which called image resampling. There is no change in spatial resolution after applying resampling process because the spatial resolution depends on properties of image capturing sensor, only the change in pixel dimension (pixel resolution). The raw images may not be of same resolution like the reference one. The image resolution of raw image may affect the accuracy of the resultant corrected image. This research study the effect of resolution of raw images with respect to the reference images on the accuracy of geometric correction process, to finally get accurate images suitable for different applications.

II. AREA OF STUDY

The available images for study area are two raw images without information about its coordinates, projection or sources of distortion from different sensors. The first image, shown in Fig. 1, is captured by IKONOS satellite sensor and the other one shown in Fig. 2, is captured by LANDSAT8 satellite sensor. Reference image acquired by remote sensing satellite (IKONOS-2), with bounded coordinates as the upper

Mohamed Tawfik, Electric and Computer Engineering Department, Military Technical College, Cairo, Egypt, 0201099968534,

Hassan Elhifnawy, Civil Engineering Department, Military Technical College, Cairo, Egypt, 0201006875547

Ayman Ragab, Civil Engineering - Public works Department, Faculty of Engineering, Ain Shams University, Cairo, Egypt, 0201223414524

Essam Hamza, Electric and Computer Engineering Department, Military Technical College, Cairo, Egypt, 0201010147947

left corner coordinates are (339924.16, 3340124.80) and the lower right corner coordinates are (347119.66, 3325676.30) which located in Cairo, Egypt. This image contains the area of study with Universal Transverse Mercator (UTM) projection, WGS84 datum and zone 36 north. Fig. 3 shows the reference image with shape layer of 20 point with red color that will be used as check points (ChPs) and their coordinates are listed in Table I and also shape layer of 4 GCPs with green colors, which are sharp defined and well distributed; to be used for transformation process in all cases of study through the research works.

Table I: Planimetric Ground Coordinates of 20 points used as check points

Check Point ID	X (MAP)	Y (MAP)
ChP. # 1	343944.7	3333179.3
ChP. # 2	346472.7	3335282.3
ChP. # 3	345623.7	3330889.3
ChP. # 4	344149.7	3334226.3
ChP. # 5	45394.66	3332933.3
ChP. # 6	343604.66	3331378.3
ChP. # 7	342166.66	3331321.3
ChP. # 8	342101.66	3329410.8
ChP. # 9	342678.66	3334365.3
ChP. # 10	341781.66	3333837.3
ChP. # 11	343871.6	3335161.3
ChP. # 12	345898.6	3332253.3
ChP. # 13	347182.6	3334338.3
ChP. # 14	345886.6	3329335.3
ChP. # 15	346166.6	3336378.3
ChP. # 16	341934.6	3333052.3
ChP. # 17	340745.6	3332008.3
ChP. # 18	340720.6	3330449.3
ChP. # 19	343313.6	3329644.3
ChP. # 20	346146.6	3334211.3



Fig. 1: Raw Image (IKONOS)



Fig. 2:Raw Image (LANDSAT8)



Fig. 3: Reference Image with distributed 20 point used as check points (red colors) & 4 GCPs with (green colors)

III. RESEARCH ALGORITHM AND METHODOLOGIES

Fig. 4 shows a schematic diagram of research algorithm. The research work flow is performed using two dimensional transformations with first order polynomial for coordinate transformation as it is the simplest form that required only four GCPs in addition, the Nearest Neighbor technique is used for intensity interpolation process for the resultant corrected images. The research implemented for testing different raw images resolutions with respect to reference image resolution.

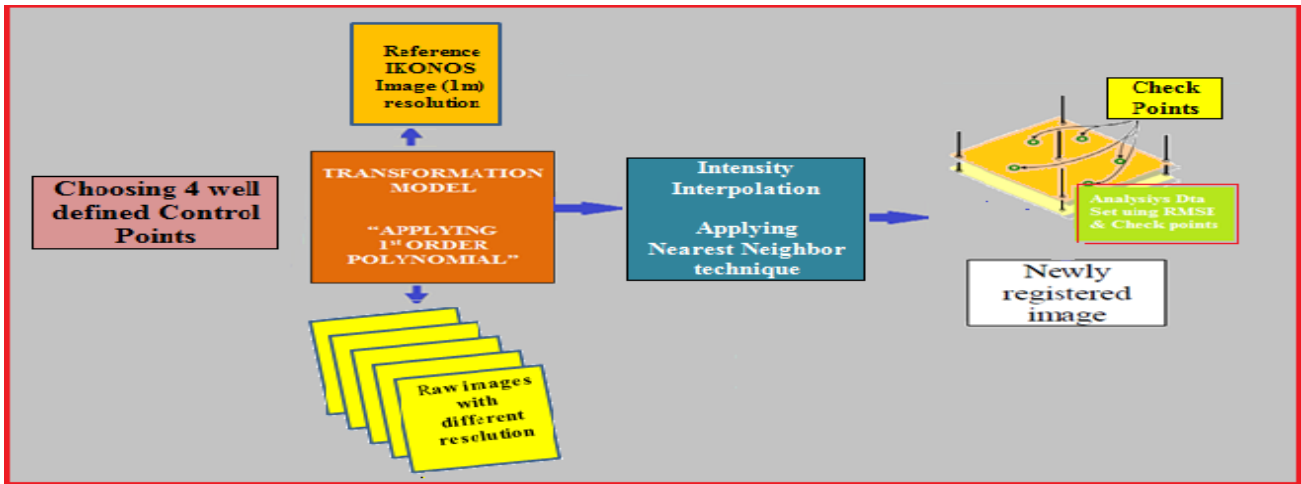


Fig. 4: A schematic algorithm of work flow

The research uses empirical approach with applying 2D mathematical transformation model with first degree of polynomial as the data do not contain elevation information. Then, Nearest Neighbor algorithm is applied for resampling process in order to preserve the original DN value of pixels of the corresponding Raw input image. The 2D transformation model with its corresponding first order polynomial form is implemented to get the transformation parameters among ground control points in the reference image and their corresponding points in the raw image. The transformation parameters consist of three main types, translation, rotation and scaling [10] [11], as shown in (1).

$$\begin{bmatrix} x \\ y \end{bmatrix} = \begin{bmatrix} a_0 & a_1 & a_2 \\ b_0 & b_1 & b_2 \end{bmatrix} \begin{bmatrix} 1 \\ X \\ Y \end{bmatrix} \quad (1)$$

Where

x, y = image coordinate

X, Y = reference coordinate

$a_0, b_0, a_1, b_1, a_2, b_2$ = translation, rotation and scaling parameters.

The accuracy of the resultant images is tested by calculating the Root Mean Squares (RMS) of the used GCPs. RMS is calculated based on the resultant vector from residuals in x and y axes of each ground control point, which expressed in pixel widths [12] [13], as shown in (2). Total Root Mean Square (TRMS) error is the combination of errors in ground control points and determined by the formula shown in (3) [12] [13]. Error contribution by point is normalized value representing each point's RMS error in relation to the TRMS error formulas shown in (4) [13] [14]. Linear errors is defined as the difference between the measured coordinate of point in the corrected image (registered) and the corresponding point in the reference image; which is simply determined as in (5) [15]. The research uses the linear errors, along with the corresponding computed TRMS of all selected check points and all used GCPs for assessing the accuracy of the resultant geometric correction model.

$$RMS_i = \sqrt{XR_i^2 + YR_i^2} \quad (2)$$

Where:

RMS_i = the RMS error for GCP_i ; XR_i = the X residual for GCP_i ; YR_i = the Y residual for GCP_i

$$TRMSE = \sqrt{1/n \sum_{i=1}^n XR_i^2 + YR_i^2} \quad (3)$$

Where:

TRMSE = total RMS error; n= the number of GCPs; i= GCP number; XR_i = the X residual for GCP_i ; YR_i = the Y residual for GCP_i

$$E_i = RMS_i / TRMS \quad (4)$$

Where:

E_i = error contribution of GCP_i ; RMS_i = the RMS error for GCP_i ; $TRMS$ = total RMS error

$$\text{Linear Error} = \sqrt{(\Delta X^2 + \Delta Y^2)} \quad (5)$$

Where:

$\Delta X = (X_{Measured} - X_{Reference})$

$\Delta Y = (Y_{Measured} - Y_{Reference})$

$X_{Measured}, Y_{Measured}$ = Coordinate of point in the corrected image (registered).

$X_{Reference}, Y_{Reference}$ = Coordinate of point in the reference image.

IV. RESEARCH ALGORITHM AND METHODOLOGIES

The experimental work is applied using Earth Resources Data Analysis System (ERDAS) Imagine Software 2015. The available data is a reference IKONOS-2 satellite image with (1.0) meter resolution, raw IKONOS with (1.0) meter resolution and raw LANDSAT8 with (15.0) meter resolution. The resampling technique is applied on the raw IKONOS image four times to generate four images with different pixel resolutions.

The Effect of Image Resolution on the Geometric Correction of Remote Sensing Satellite Images

The research algorithm is implemented through six cases of study as shown in Fig. 5. The geometric correction is applied by using same reference image with (1.0) meter resolution and six images with different pixel resolutions, 1.0

m (IKONOS Image), 4.0 m (IKONOS Image), 7.0 m (IKONOS Image), 10.0 m (IKONOS Image), 15.0 m (IKONOS Image) and the seven case as 15.0 m (LANDSAT Image).

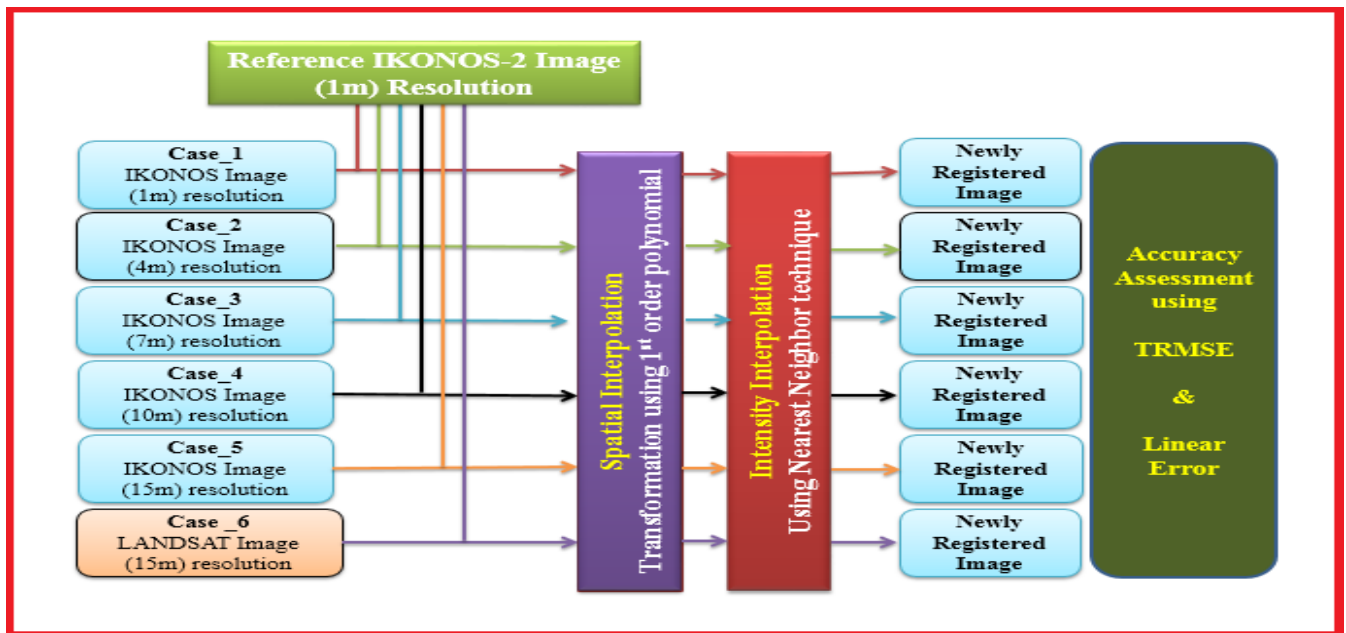


Fig. 5: A flow chart of work flow of that research

V. RESULTS OF SEVEN CASES USING DATA FROM IKONOS & LANDSAT SATELLITE SENSOR

Firstly, the available IKONOS satellite images data is one raw image of 1.0 m resolution, four images are generated from the raw image with different pixel resolution; The four generated images with pixel resolution larger than the reference image (4.0 m, 7.0 m, 10.0 m and 15.0 m) respectively. These will constitute the five study cases of IKONOS satellite image with different pixel resolution. Secondly, the available LANDSAT8 satellite images data is one raw image of 15.0 m resolution that is downloaded from USGS Earth Explorer (<http://earthexplorer.usgs.gov>), which

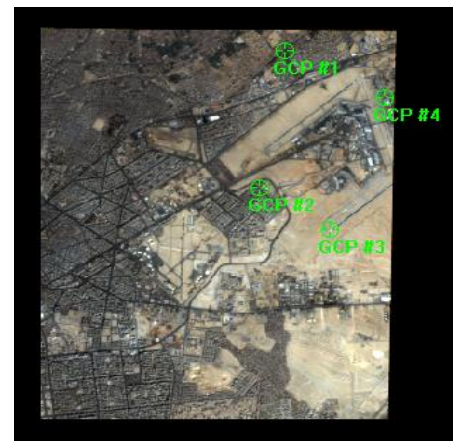
considered as commercial free image source. This will constitute the sixth case of LANDSAT8 satellite image that can be used for comparing its results with the result of the generated IKONOS image of pixel resolution 15.0 m. The research studies the effect of image resolution on the accuracy of geometric correction using different pixel resolution of raw images with respect to reference IKONOS-2 image, which is in 1.0 m constant resolution in all cases of study. The distribution of GCPs in all six cases of study is the same as shown in Fig. 6. The RMS errors at each GCP in the six study cases are listed in Table II. Also, the linear errors at the ten Check points, which appeared in both reference and raw images in each of six study cases, are listed in Table III.



Distribution of GCP in Raw IKONOS images with different resolution [case1:case5]



Distribution of GCP in Raw LANDSAT8 Image [case 6]



Distribution of GCP in Reference IKONOS-2 Image

Fig. 6: The disposition for GCP in all six study cases

Table II: The RMS error at each GCP in all study cases

Case 1 (1.0 m) IKONOS					Case 2 (4.0 m) IKONOS				
GCP ID	Residual		Result		GCP ID	Residual		Result	
	X	Y	RMSE	Contrib.		X	Y	RMSE	Contrib.
1	-0.037	0.058	0.069	0.863	1	0.041	0.067	0.079	0.863
2	0.050	-0.079	0.094	1.177	2	-0.056	-0.092	0.108	1.177
3	-0.047	0.075	0.088	1.111	3	0.053	0.087	0.102	1.111
4	0.034	-0.054	0.063	0.798	4	-0.038	-0.062	0.073	0.798
Case 3 (7.0 m) IKONOS					Case 4 (10.0 m) IKONOS				
GCP ID	Residual		Result		GCP ID	Residual		Result	
	X	Y	RMSE	Contrib.		X	Y	RMSE	Contrib.
1	0.063	-0.115	0.131	0.864	1	0.202	0.343	0.398	0.863
2	-0.085	0.156	0.178	1.175	2	-0.275	-0.468	0.543	1.176
3	0.081	-0.148	0.168	1.111	3	0.260	0.442	0.512	1.111
4	-0.058	0.106	0.121	0.800	4	-0.187	-0.317	0.368	0.798
Case 5 (15.0 m) IKONOS					Case 6 (15.0 m) LANDSAT8				
GCP ID	Residual		Result		GCP ID	Residual		Result	
	X	Y	RMSE	Contrib.		X	Y	RMSE	Contrib.
1	-0.312	-0.297	0.430	0.863	1	0.27	0.385	0.471	0.863
2	0.425	0.405	0.587	1.176	2	-0.369	-0.525	0.642	1.177
3	-0.402	-0.382	0.555	1.112	3	0.349	0.496	0.606	1.111
4	0.288	0.275	0.398	0.798	4	-0.250	-0.356	0.435	0.798

Table III: Linear Error at the available Ten Check Points in all study cases

Case 1 (1.0 m) IKONOS				Case 2 (4.0 m) IKONOS			
ChP. ID	ΔX	ΔY	Linear Error	ChP. ID	ΔX	ΔY	Linear Error
1	-3.16	-0.8	3.2596	1	4.34	0.7	4.3960
2	-5.16	2.2	5.6094	2	-3.66	-2.3	4.3226
3	-0.16	1.2	1.2106	3	1.34	2.7	3.0142
4	2.84	-3.81	4.7520	4	11.34	1.69	11.4652
5	-3.16	3.2	4.4972	5	-1.66	2.7	3.1694
6	-0.16	-1.8	1.8070	6	0.34	-2.3	2.3249
11	-2.16	-4.8	5.2636	11	5.34	-1.3	5.4959
12	1.84	0.2	1.8508	12	-5.66	6.7	8.7707
13	-4.16	1.98	4.6071	13	-5.66	1.7	5.9097
20	-4.16	2.21	4.7105	20	-4.06	2.74	4.8980
Case 3 (7.0 m) IKONOS				Case 4 (10.0 m) IKONOS			
ChP. ID	ΔX	ΔY	Linear Error	ChP. ID	ΔX	ΔY	Linear Error
1	-2.15	7.19	7.5045	1	9.36	-12.3	15.4564
2	-10.17	4.19	10.9993	2	-18.65	4.7	19.2331
3	-8.15	8.19	11.5541	3	-19.66	-2.3	19.7941
4	-11.16	10.18	15.1055	4	-10.75	12.28	16.3205
5	-3.31	8.39	9.0193	5	-17.09	3.69	17.4838
6	8.85	2.19	9.1169	6	-0.66	-21.31	21.3202
11	-6.16	-14.8	16.0307	11	-8.0	-44.37	45.0854
12	-10.17	9.19	13.7071	12	-14.65	3.7	15.1100
13	-13.16	10.2	16.6500	13	-18.76	9.32	20.9475
20	-6.12	-3.54	7.0701	20	-12.66	5.68	13.8758
Case 5 (15.0 m) IKONOS				Case 6 (15.0 m) LANDSAT8			

ChP. ID	ΔX	ΔY	Linear Error	ChP. ID	ΔX	ΔY	Linear Error
1	-28.15	4.21	28.4630	1	-12.17	-9.83	15.6441
2	23.84	16.19	28.8177	2	-20.18	2.2	20.2995
3	-27.25	29.19	39.9326	3	-11.16	0.19	11.1616
4	-53.86	-22.36	58.3169	4	7.84	8.18	11.3304
5	-8.09	25.42	26.6762	5	-22.18	11.18	24.8383
6	-48.22	-24.83	54.2374	6	-32.17	6.27	32.7753
11	-30.12	-42.82	52.3523	7	-19.17	-56.84	59.9856
12	-2.25	30.09	30.1740	10	-9.12	-52.8	53.5818
13	48.97	-0.04	48.9700	13	-10.16	-13.8	17.1366
20	35.03	7.3	35.7825	16	-12.14	-62.84	64.0019

VI. ACCURACY EVALUATION

As stated before, the accuracy assessment depends mainly on the TRMS of check points positioning, which is simply again computed as shown in (6). Here, Table IV listed the total root

mean square errors in easting and northing direction as well as in positioning for all ground and check points in six cases of study.

$$\begin{aligned}
 TRMS X &= \sqrt{\left(\sum_i^n \Delta X^2 / n\right)} \\
 TRMS Y &= \sqrt{\left(\sum_i^n \Delta Y^2 / n\right)} \\
 TRMS P &= \sqrt{((TRMS X)^2 + (TRMS Y)^2)}
 \end{aligned}
 \tag{6}$$

Where:

TRMS X is Total Root mean square errors in Easting direction for ground and check points in each case of study

TRMS Y is Total Root mean square errors in Northing direction for ground and check points in each case of study

TRMS P is Total Root mean square errors in positioning for ground and check points in each case of study

ΔX is the different between source and retransformed GCP coordinate in easting direction & also different between Reference and measured Check points coordinate in easting direction

ΔY is the different between source GCP and retransformed GCP coordinate in northing direction & also different between Reference and measured Check points coordinate in northing direction

n = number of ground and check points

Table IV: Total RMS errors in Easting & Northing for GCPS and check points used in six cases of study

Name	Total RMSE For used GCPs			Total RMSE For used ChPs		
	TRMS X	TRMS Y	TRMS P	TRMS X	TRMS Y	TRMS P
Case 1 (1.0 m) IKONOS	0.0425	0.0672	0.0795	3.1205	2.5845	4.0518
Case 2 (4.0 m) IKONOS	0.0478	0.0781	0.0916	5.2398	2.9237	6.0003
Case 3 (7.0 m) IKONOS	0.0726	0.1330	0.1515	8.6041	8.5744	12.1471
Case 4 (10.0 m) IKONOS	0.2338	0.3976	0.4612	14.2156	17.0256	22.1800
Case 5 (15.0 m) IKONOS	0.3613	0.3440	0.4989	34.5431	23.8471	41.9751
Case 6 (15.0 m) LANDSAT8	0.3137	0.4464	0.5456	15.4468	30.3837	34.0848

Fig. 7 shows a quick analysis in graphical representation as bars chart of linear errors at the common check points in all cases of study. From the evaluation of linear error magnitude in all study cases, it's logically clear that linear errors at each check points are increased with the degradation of pixel resolution in the raw images. Also, points near the chosen ground control point give a significant improvement in the corresponding linear error, as in the case of check point (3) & (6) in **Error! Reference source not found.**, especially in raw

image resolution nearly the same of the reference image. Finally, image from LANDSAT8 is preferable than image generated from IKONOS for applying geometric correction, although they have same resolution, 15.0 m, as quite clear by comparing both case (5) and case (6) at all common check points. Because resampling process may cause errors due to change in the original (DN) values of the image, which may cause change in feature position.

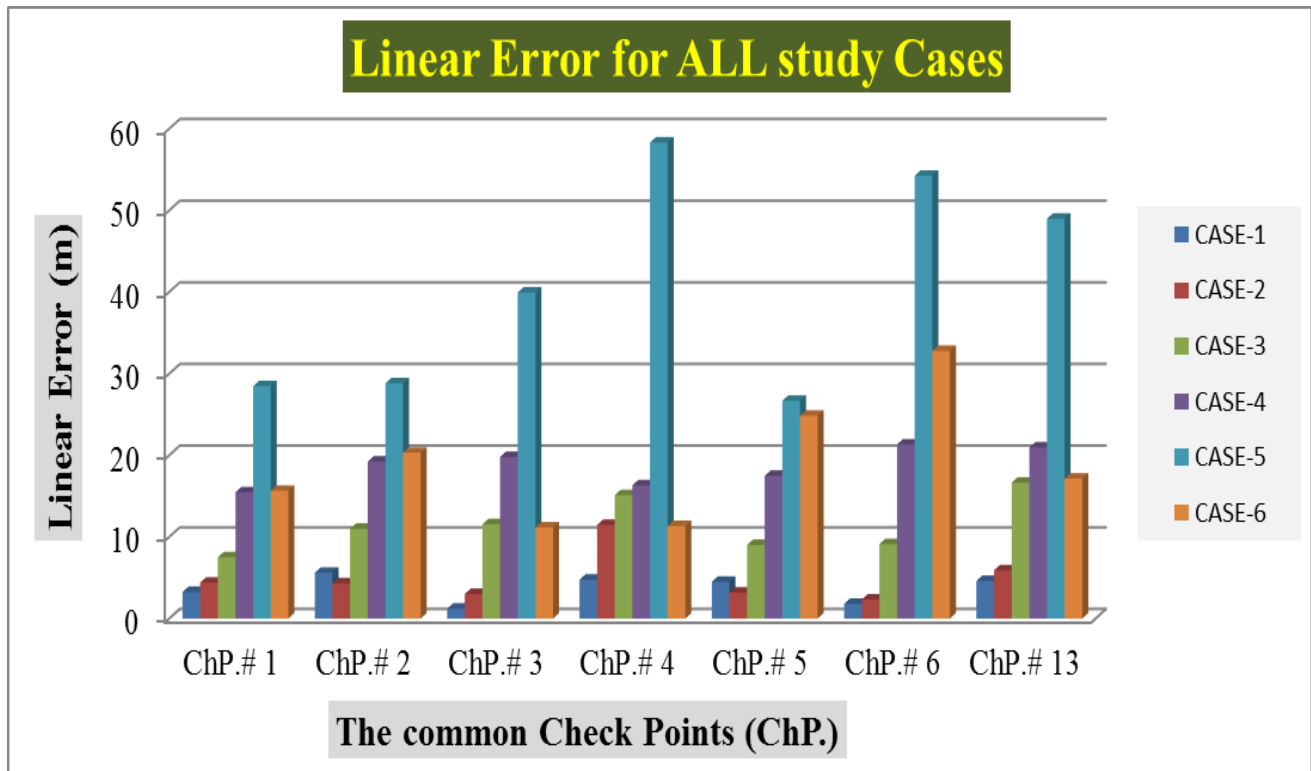


Fig. 7: Linear Error in common check points in all study cases

VII. CONCLUSION

Image geometric correction depends on the available georeferencing data, ground control points, reference image, and a map. Choosing resolution of raw image with respect to reference image resolution is important factor that affects the accuracy of geometric correction. The research ended up to when doing a registration, you should register two images with same resolution or use the reference image with high resolution than the raw image resolution to get accurate results. As choosing the image resolution near or the same as reference image resolution will help in sharply define the features in the two images, which affect the accuracy of correction process. From experimental results, the first two cases give acceptable results; so the resolution of raw image up to four or five times the reference image resolution gives acceptable results. Choosing image resolution of raw images depends on the required accuracy of the application as city development projects need accuracy lower than database updating and target tracking. Accuracy of the resultant image that is expressed by RMS and linear error values can be taken in consideration in selecting raw image resolution of the available data, which will be suitable for specific applications. Images after making pixel resolution greater than four times its spatial resolution will give greater errors because the original DN values are changed during resampling process, which may cause change in feature

position, so when select these feature it's not sharply defined. LANDSAT images can be used for same applications that need same resolution even if the available reference data are captured from different sources. This tends to get acceptable results with saving cost and time to get data of same resolution from same sensors. Targets tracking application as guided missiles need linear errors have to be small as possible. In this case, it is recommended to use raw images of same or higher resolution than reference image even if it needs high costs.

REFERENCES

- [1] M. Hosseini and J. Amini, "Comparison between 2-D and 3-D transformations for geometric correction of IKONOS images," *ISPRS, Hannover*. www.isprs.org/publications/related/hannover05/paper, 2005.
- [2] F. Eltohamy and E. Hamza, "Effect of ground control points location and distribution on geometric correction accuracy of remote sensing satellite images," in *13th International Conference on Aerospace Sciences & Aviation Technology (ASAT-13)*, 2009.
- [3] S. S. Baboo and M. R. Devi, "Geometric correction in recent high resolution satellite imagery: a case study in Coimbatore, Tamil Nadu," *International Journal of Computer Applications*, vol. 14, pp. 32-37, 2011.
- [4] T. Toutin, "State-of-the-art of geometric correction of remote sensing data: a data fusion perspective," *International Journal of Image and Data Fusion*, vol. 2, pp. 3-35, 2011.

- [5] T. Toutin, "Review article: Geometric processing of remote sensing images: models, algorithms and methods," *International Journal of Remote Sensing*, vol. 25, pp. 1893-1924, 2004.
- [6] D. A. V. P. a. P. M. P. Devangi B . Thakkar, ""Geometric Distortion and Correction Methods for Finding Key Points:A Survey", " " *International Journal for Scientific Research and Development* ", vol. Vol. 4 , , p. 4, 2016.
- [7] J. A. Richards and J. Richards, *Remote sensing digital image analysis* vol. 3: Springer, 1999.
- [8] S. Suri, S. Türmer, P. Reinartz, and U. Stilla, "Registration of high resolution SAR and optical satellite imagery in urban areas," 2009.
- [9] A. Habib and R. Al-Ruzouq, "Semi-automatic registration of multi-source satellite imagery with varying geometric resolutions," *Photogrammetric Engineering & Remote Sensing*, vol. 71, pp. 325-332, 2005.
- [10] M. V. Zoej, A. Mansourian, B. Mojaradi, and S. Sadeghian, "2D geometric correction of IKONOS imagery using genetic algorithm," in *International Archives of Photogrammetry and Remote Sensing and Spatial Information Sciences*, 2002.
- [11] K. S. OO, "Reliable Ground Control Points for Registration of High Resolution Satellite Images," 2010.
- [12] K.-t. Chang, *Introduction to geographic information systems*: McGraw-Hill Higher Education Boston, 2006.
- [13] H. E. Mohamed Tawfeik , Essam Hamza and Ahmed Shawky "Determination of suitable requirements for Geometric Correction of remote sensing Satellite Images when Using Ground Control Points," *International Research Journal of Engineering and Technology* vol. 03, p. 54:63, 2016
- [14] "ERDAS Field Guide™ Fifth Edition, Revised and Expanded, CHAPTER 9 "Rectification", " 2015.
- [15] M. E. A. Babiker and S. K. Y. Akhadir, "The Effect of Densification and Distribution of Control Points in the Accuracy of Geometric Correction," 2016.



Eng. Mohamed Tewfik; graduated from Electric and Computer Engineering Department, Military Technical College, Cairo, Egypt in 2010.